A short introduction to numerical methods used in cosmological N-body simulations

Wojciech Hellwing[1,2]

1. Institute for Computational Cosmology, Department of Physics, Durham University, South Road, Durham DH1 3LE, UK
2. Interdisciplinary Centre for Mathematical and Computational Modeling (ICM), Univesity of Warsaw, ul. Pawińskiego 5a, Warsaw, Poland

We give a short introduction to modern numerical methods commonly used in cosmological N-body simulations. First, we present some simple considerations based on linear perturbation theory which indicate the necessity for N-body simulations. Then, based on a working example of the publicly available GADGET-2 code, we describe particle mesh and Barnes-Hut oct-tree methods used in numerical gravity N-body solvers. We also briefly discuss methods used in an elementary hydrodynamic implementation used for baryonic gas. Next, we give a very basic description of time integration of equations of motion commonly used in N-body codes. Finally we describe the Zeldovitch approximation as an example method for generating initial conditions for computer simulations.

1 Introduction

Observations of the Cosmic Microwave Background (CMB) have pinned down the state of the universe when it was only $\sim 350,000$ years old. At this early stage the universe was very smooth, with different regions exhibiting very similar temperatures and densities. Fluctuations around homogeneity were very small, yet important: due to gravitational instability, the initially overdense regions grew into the galaxies, galaxy clusters and cosmic voids observed today. Because the initial conditions are known to a very good precision, modelling and understanding the growth of large-scale structure of the Universe is a well-defined problem. However, it is an intrinsically difficult problem because gravity is inherently nonlinear and the physics is complicated. The resulting large-scale structure creates a rich hierarchy spanning many orders of magnitude in density. Such a system is hard to study in a simple computational framework, but in principle it is a solvable problem. In this context, numerical simulations play a dual role. They provide insight into the ways in which the initially smooth universe transformed into one with the magnificent structure observed today. They also enable cosmologists to compare cosmological models and theories with ever-more powerful data sets obtained from large telescopes and cosmic probes. Experiments planned for the near future are challenging the computational cosmology community to produce simulations sufficiently sophisticated and accurate to extract the relevant dark sector (dark matter and dark energy) information from a universe with many layers of complexity.

In this contribution we will present a short introduction to basic methods and principles that constitute the basis of today's state-of-the-art cosmological numerical simulations.

2 The need for numerical simulations: break down of linear perturbation theory

After the epoch of cosmic inflation, all fluctuations of the gravitational potential and matter density were very small. The observed fluctuations of the microwave background radiation are of the order of 10^{-5} (Bennett et al., 1994, 1996; Komatsu et al., 2010; Planck Collaboration et al., 2014), while the present day density contrast can reach $\sim 10^5$ in centres of galaxies and 10^3 in galaxy clusters. The process of cosmic structure formation consists of many orders of magnitude of growing density contrast. Some part of this process can be described by linear perturbation theory, which gives a valid picture of the evolution of density field perturbations as long as the amplitude of these perturbations is small (i.e. $\Delta\rho/\rho \lesssim 1$). We begin by writing down the three basic equations which describe density field fluctuations. The continuity equation:

$$\left(\frac{\partial\rho}{\partial t}\right)_{\vec{r}} + \vec{\nabla}_{\vec{r}} \cdot (\rho\vec{u}) = 0\,, \tag{1}$$

the Euler equation:

$$\frac{\mathrm{d}\vec{u}}{\mathrm{d}t} = \left(\frac{\partial\vec{u}}{\partial t}\right)_{\vec{r}} + (\vec{u}\cdot\vec{\nabla}_{\vec{r}})\vec{u} = -\vec{\nabla}_{\vec{r}}\Phi - \frac{1}{\rho}\vec{\nabla}_{\vec{r}}p\,, \tag{2}$$

and the Poisson one:

$$\vec{\nabla}\times\Phi = 0\,, \quad \nabla^2_{\vec{r}}\Phi = 4\pi G\rho\,. \tag{3}$$

Here $u(t)$ depicts velocity, while Φ is the gravitational potential. p is fluid pressure, ρ its density. G stands for the usual Newtonian gravitational constant and t is the average cosmic time. Superscript $\vec{r}$ indicates that we express the relevant quantities in physical coordinates. We will now introduce a small density perturbation:

$$\rho(\vec{r},t) = \rho_0(t)[1+\delta(\vec{r},t)]\,, \tag{4}$$

where the subscript 0 denotes the non-perturbed averaged background density at time t. The matter in the vicinity of a density perturbation will have some peculiar velocity $\vec{v}$, i.e. a velocity not related to the Hubble flow. Thus the full velocity of a material test particle will be:

$$\vec{u} = \frac{\mathrm{d}(a\vec{r})}{\mathrm{d}t} = \dot{a}\vec{r} + \vec{v}(\vec{r},t)\,, \tag{5}$$

where $v = a\dot{\vec{r}}$ denotes the peculiar velocity and $\dot{a}\vec{r}$ is the velocity related to the universal expansion. The density fluctuation will also induce a peculiar gravitational potential ϕ, which is different from the potential of the smoothed unperturbed background:

$$\Phi = \Phi_0 + \phi\,. \tag{6}$$

We will now analyse the above equations using the perturbed quantities δ, ϕ, v, instead of the quantities describing the unperturbed averaged background ρ, Φ and

u. We start by rewriting the pressure term in the Euler equation using the definition of the acoustic velocity

$$\frac{1}{\rho}\vec{\nabla}_{\vec{r}}p = \frac{1}{a\rho_0(1+\delta)}\frac{\partial p}{\partial \rho}\vec{\nabla}\rho_0(1+\delta) = \frac{1}{a(1+\delta)}c_s^2\vec{\nabla}\delta\,, \tag{7}$$

where by c_s we have marked the speed of sound. The next step in our analysis consists of changing the coordinate system from the physical $\vec{r}$ to comoving coordinates $\vec{x}$. In this simple way we will naturally include in our equations effects related to the expansion of the Universe. The comoving and physical coordinates are connected by two relations:

$$\vec{x} = \frac{\vec{r}}{a(t)}\,, \quad \nabla_{\vec{x}} = a\nabla_{\vec{r}}\,. \tag{8}$$

The conversion of a time derivative of an arbitrary function f taken at a point $\vec{r}$ to a time derivative of this function at the defined point $\vec{x}$ needs to include the Hubble flow:

$$\left(\frac{\partial f}{\partial t}\right)_{\vec{r}} + H\vec{r}\cdot\vec{\nabla}_{\vec{r}}f = \left(\frac{\partial f}{\partial t}\right)_{\vec{x}}\,. \tag{9}$$

For simplicity and clarity, from now on we will omit the subscript $\vec{x}$. After changing the coordinates in which we express our equations, we can simplify further by subtracting the equations for unperturbed quantities from the equations describing perturbed quantities. This results in:

$$\frac{\partial\delta}{\partial t} + \frac{1}{a}\vec{\nabla}\cdot[(1+\delta)\vec{v}] = 0\,, \tag{10}$$

$$\frac{\partial\vec{v}}{\partial t} + \frac{\dot{a}}{a}\vec{v} + \frac{1}{a}(\vec{v}\cdot\vec{\nabla})\vec{v} = -\frac{1}{a}\vec{\nabla}\phi - \frac{1}{a(1+\delta)}c_s^2\vec{\nabla}\delta\,, \tag{11}$$

$$\nabla^2\phi = 4\pi G\rho_0 a^2\delta\,. \tag{12}$$

Now we will linearise the continuity and Euler equations by removing all terms which are smaller than the small perturbed quantities δ, ϕ and $\vec{v}$. After this operation both equations take the form:

$$\frac{\partial\delta}{\partial t} + \frac{1}{a}\nabla\cdot\vec{v} = 0 \tag{13}$$

$$\frac{\partial\vec{v}}{\partial t} + \frac{\dot{a}}{a}\vec{v} + \frac{1}{a}\nabla\phi + \frac{1}{a}c_s^2\vec{\nabla}\delta = 0\,. \tag{14}$$

We can eliminate the peculiar velocity $\vec{v}$ by subtracting $1/a$ times the divergence of the second equation from the first equation differentiated with respect to time. Now, by substituting in the linearised Poisson equation, we can finally obtain:

$$\ddot{\delta} + 2\frac{\dot{a}}{a}\dot{\delta} - 4\pi G\rho_0\delta - \frac{c_s^2}{a^2}\nabla^2\delta = 0\,, \tag{15}$$

where the dots mark the derivatives taken with respect to cosmic time. The above equation describes the time evolution of density field perturbations for an arbitrary background Friedmann-Lemaître model, provided that the fluctuations are small ($\delta \ll 1$). As long as this condition holds, we can express the spatially-fluctuating

density field δ as a sum of Fourier modes. Each mode will be characterised by a wave number k or the corresponding wavelength λ (so that $k\lambda = 2\pi$) and its amplitude δ_k. The evolution equation (15) can be also written for a single Fourier mode. It will take a simpler form, since in Fourier space differentiation with respect to the spatial coordinate is equal to multiplying by ik. Hence, if

$$\delta(\vec{x}) = \sum \delta_k e^{-ik\cdot\vec{x}}\,, \tag{16}$$

then

$$\vec{\nabla}\delta(\vec{x}) = \sum -ik\delta_k e^{-ik\cdot\vec{x}}\,, \quad \nabla^2\delta(\vec{x}) = \sum k^2\delta_k e^{-ik\cdot\vec{x}}\,. \tag{17}$$

Finally the single Fourier mode evolution equation takes the form:

$$\frac{\partial^2\delta_k}{\partial t^2} + 2\frac{\dot{a}}{a}\frac{\partial\delta_k}{\partial t} + \left(\frac{c_s^2k^2}{a^2} - 4\pi G\rho_0\right)\delta_k = 0\,. \tag{18}$$

This equation has two general types of solutions, depending on the sign of the term in parentheses:

1. If $c_s^2k^2/a^2 > 4\pi G\rho_0$, then the solutions for δ_k are sinewaves, and so, for an arbitrary point in time and space, the local density contrast oscillates in time. The physical interpretation is the following: if the term $c_s^2k^2/a^2$ dominates, then forces related to pressure are big enough to effectively oppose the force of gravity. The perturbation cannot grow in time, but the gravity acts as a force inducing harmonic oscillations.

2. If the term in the parentheses is negative, then the solutions describing δ_k will not be harmonic oscillators but functions monotonic in time. These monotonic solutions describes a density contrast growing or decaying in time. Hence in this case the forces of gravity are strong enough to overcome the internal pressure and induce gravitational collapse of a perturbation. Therefore, the monotonic growth of δ_k can lead to formation of bound structures at late times.

3. The borderline case between the two above solutions is when the term in parentheses is exactly equal to zero. The related perturbation scale is called the Jeans scale $k_J = a/c_s\sqrt{4\pi G\rho_0}$. The equivalent Jeans length is $\lambda_J = 2\pi/k_J$ and the Jeans mass (the mass enclosed by the perturbation) will be $M_J = \rho_0\lambda_L^3$.

Using the standard Friedmann equation for the time evolution of the cosmic scale factor $a(t)$ together with the density perturbation evolution equation (18), we can infer the growth of the dark matter (DM) density field fluctuations for different evolution phases of a ΛCDM universe. We can treat the dark matter as non-relativistic pressureless fluid (dust solutions), and hence set the speed of sound term to zero $c_s^2 = 0$.

2.1 Growth of density fluctuations in the radiation era

During the radiation era, the biggest contribution to energy density of the Universe comes from photons which, being a relativistic fluid, do not cluster. This means that the last term in equation (18) vanishes, since $\delta_{tot} = \delta_{DM} + \delta_{barions} + \delta_{photons} \approx$

$\delta_{photons} \approx 0$. During the radiation era, the time dependence of the scale factor during the radiation era is $a \propto t^{1/2}$, hence $H = 1/(2t)$ (see more details in Dodelson, 2003). Therefore the density evolution equation reduces to:

$$\ddot{\delta_k} + 2H\dot{\delta_k} = \ddot{\delta_k} + \frac{1}{t}\dot{\delta_k} = 0\,. \tag{19}$$

This equation has two solutions:

$$\delta_k \propto A \times \text{const} + B \ln t\,. \tag{20}$$

This indicates that the density fluctuations of DM can grow, at best, logarithmically in time, which is slow growth. The density perturbations of baryons, which are coupled to photons via Thompson scattering, are oscillating and hence do not grow at all. This indicates that, during the radiation dominated era, the large-scale structure cannot grow effectively.

2.2 Growth of density fluctuations in the matter era

During this phase the term related to matter density dominates in the Friedmann equation. Hence we can approximate this phase using the solution for the Einstein-de Sitter (EdS) universe, for which $\Omega_m = 1$. This simplifies many calculations. Since now $a \propto t^{2/3}$, hence for EdS model the Hubble function is $H = 2/(3t)$. Using $\rho_0 = \rho_c = 3H^2/8\pi G$, the evolution equation assumes:

$$\ddot{\delta_k} + \frac{4}{3t}\dot{\delta_k} = \frac{2}{3t^2}\delta_k\,. \tag{21}$$

The general solution of the above is:

$$\delta_k \propto At^{2/3} + Bt^{-1}\,, \tag{22}$$

where A and B are constants. Thus we have one solution growing in time and one decaying. The growing solution will eventually dominate. Hence, the density fluctuations of DM during this era grow proportionally to the scale factor $\delta_k \propto a$. This solution has important implications. Firstly, it means that the fluctuations grow quickly enough to form the large-scale structure. Secondly, we note that the growth rate does not depend on k, hence all the modes grow with the same rate. This means that a region of the Universe whose density perturbation $\delta(\vec{x})$ is described by a sum of Fourier modes each with its own amplitude δ_k also grows as $\propto a$.

2.3 Growth of density fluctuations in Λ dominated era

The Friedman equation takes the simpler form

$$H^2 \approx H_0^2\Omega_\Lambda\,, \tag{23}$$

hence $H = \text{const}$. The contribution of Ω_m to the Friedmann equation is negligible, since Ω_Λ is bigger than the contribution of all other forms of matter-energy in the Universe. This implies $\rho_0 \sim 0$ which, substituted into the evolution equations, leads to:

$$\ddot{\delta_k} + 2H\dot{\delta_k} = 0\,. \tag{24}$$

The general solutions of this equation take the form:

$$\delta_k \propto A \times \text{const} + B\, e^{-2Ht}\,. \tag{25}$$

The analysis of the above solution leads to a conclusion that, as soon as the Λ term starts to dominate in the Friedmann equation, the structure formation process ceases at scales where the smoothed density contrast is $\delta \lesssim 1$. At the present day this scale is $\sim 20-30$ Mpc, which is the characteristic scale for superclusters and cosmic voids. Freezing out of structure formation on those scales does not mean that the structures for which the density contrast is large $\delta \gg 1$ have also stopped growing or evolving, such perturbations will still evolve until they reach the virialised state, i.e. exchange their excess gravitational potential energy for the kinetic energy of random thermal motions.

The above analysis of the cosmic structure formation process in the linear regime clearly indicates that the large-scale structure in a ΛCDM universe can grow effectively only when nonrelativisitc matter is the dominant from of energy-density. It is satisfied for scale factors in the range of $10^{-4} \lesssim a \lesssim 0.7$. Hence for a universe of a total age of 13.7 billion of years, the cosmic large-scale structure experiences ~ 10 billion of years of effective growth. During that time the structure grows fast, and so even very small initial density contrast can quickly reach high values. For $\delta_k \gg 1$, even the higher-order perturbation theory breaks down. Hence perturbations on scales relevant to galaxy formation and evolution quickly become non-linear. Thus the computerized numerical simulations are the only effective way to model and study the structure formation process into the non-linear regime.

3 The cosmological numerical N-body simulations

Numerical N-body simulations remain one of the most important tools of modern theoretical cosmology. Numerical N-body algorithms running on supercomputers allow study of non-linear gravitational and hydrodynamical evolution of complex particle systems. There is a great variety of cosmological N-body codes, algorithms and related numerical techniques, but in the essence all these different solutions model the time evolution of a given system by finding and following particles' trajectories, accounting for their mutual gravitational and hydrodynamical interactions. The quality of any cosmological N-body code is based on two basic requirements: (1) – generation of adequate and accurate initial conditions (IC), which are the initial positions and velocities for particles and (2) – solving as precisely as possible the equations of motion that determine particle trajectories.

For the purpose of this lecture we will use the GADGET-2 code (*GAlaxies with Dark matter and Gas intEracT*) as our working example of a cosmological N-body code. GADGET-2 was created by Volker Springel (Springel, 2005) and is publicly available [1]. It is a hybrid code which uses the combined algorithms of spatial oct-tree and particle mesh to solve the gravity and the *Smooth Particle Hydrodynamic* (SPH) method for modelling the baryonic hydrodynamical forces.

[1] `http://www.mpa.mpa-garching.mpg.de/gadget/`

3.1 Numerical gravity

Because the number density of baryons and DM particles is very high, we can describe the system whose gravitational evolution we want to model, by a single particle distribution function:

$$f = f(\mathbf{x}, \mathbf{v}, t)\,. \tag{26}$$

The function f describes the mass density in the particles' phase space. We assume that the system consists of a very large number of particles, so the local mutual scattering of particles can be neglected and the system reacts only to the resulting gravitational field. Thus we are describing a self-gravitating collisionless fluid. The time evolution of the distribution function (26) for such a system follows the collisionless Boltzmann equation (Boltzmann, 1872):

$$\frac{\mathrm{d}f}{\mathrm{d}t} \equiv \frac{\partial f}{\partial t} + \mathbf{v}\frac{\partial f}{\partial \mathbf{x}} - \frac{\partial \Phi}{\partial \mathbf{x}}\frac{\partial f}{\partial \mathbf{v}} = 0\,, \tag{27}$$

where the self-consistent potential Φ is the solution of the Poisson equation:

$$\nabla^2\Phi(\mathbf{x}, t) = 4\pi G \int f(\mathbf{x}, \mathbf{v}, t)\mathrm{d}\mathbf{v}\,. \tag{28}$$

The equations (27) and (28) make the Poisson-Vlasov system, in which the phase-space is conserved along each characteristic (i.e. a particle's orbit). It is very difficult to solve this system directly using classical finite difference methods. For a large number of particles belonging to a non-linear system it is, in practice, impossible. The standard N-body approach (used also in the GADGET-2 code) is based on using a finite number of particles to sample the underlying continuous distribution function f. This is, in at its core, a Monte-Carlo like method.

We create a discrete system of N particles moving approximately along the characteristics of the base system. For such scheme we can write a new system of equations:

$$\ddot{\mathbf{x}}_i = -\nabla\Phi(\mathbf{x}_i)\,, \tag{29}$$

$$\Phi(\mathbf{x}) = -G\sum_{j=1}^{N}\frac{m_j}{(\mathbf{x}-\mathbf{x}_j)^2 + \varepsilon^2}\,. \tag{30}$$

The ε parameter appearing in the denominator under the sum over all particles is the so-called gravitational force softening parameter. It is introduced to ensure that the resulting dynamics of the system are purely collisonless. The presence of this term brings three significant benefits:

1. it prevents dispersion of particles approaching each other at high angles and the creation of self-bounded pairs,
2. makes the two-body relaxation time big enough,
3. allows integration of the system via lower-order integration methods (numerical thriftiness).

Gravitational softening, in addition to the above-mentioned benefits, has one important disadvantage: for inter-particle separations $r \lesssim \varepsilon$ the computed force becomes

non-Newtonian. Hence often the value of this parameter is identified as the force resolution limit of a given N-body simulation. The spatial scale of ε sets the higher limit of a numerical experiment's dynamical range, at the same time it also defines the limit down to which a given N-body system carries reliable physical information.

There are various methods which allow solution of the N-body system of equations (29) and (30), each with its own advantages and disadvantages. As we have already mentioned, GADGET-2 is a hybrid code which implements two different methods to find final solutions of the Poisson-Vlasow system. On short scales it uses the spatial oct-tree algorithm to find forces exerted by nearby particles. The tree method has very good resolution and force accuracy, however it is computationally and memory-wise expensive, especially at early stages of simulation when the simulated system is very homogeneous. The second method, the particle mesh, is simpler and faster, but for small spatial separations is not accurate. By combining these two methods, one can achieve simultaneously impressive speed and accuracy of calculations. We will now look closer at these two algorithms.

3.1.1 Particle mesh method

The particle mesh method (Hockney & Eastwood, 1981) exploits the fact, that the Poisson equation for gravitational potential can be found in the real space by convolving the density with the Green's function:

$$\Phi(\mathbf{x}) = \int \mathcal{G}(\mathbf{x}-\mathbf{x}')\rho(\mathbf{x})\mathrm{d}\mathbf{x}' \,. \tag{31}$$

The choice of the particular Green's function from $\mathcal{G}$ depends on whether we consider periodic or vacuum boundary conditions. In the Fourier space the convolution is replaced by a simple multiplication

$$\widehat{\Phi(\mathbf{k})} = \widehat{\mathcal{G}(\mathbf{k})} \cdot \widehat{\rho(\mathbf{k})} \,. \tag{32}$$

To obtain $\rho(\mathbf{x})$ we place into the computational domain a regular 3D mesh with M^3 cubical cells, so each cell has a width of h. All the particles are assigned a special "shape" function $S(x)$. Each cell with a centre $\mathbf{x}_m (1 \leq m \leq M^3)$ gets a contribution of a fractional mass of particle that overlaps with that cell. The mass contribution for a given cell is given by:

$$W(\mathbf{x}_m - \mathbf{x}_i) = \int_{\mathbf{x}_m - \frac{h}{2}}^{\mathbf{x}_m + \frac{h}{2}} S(\mathbf{x}' - \mathbf{x}_i)\mathrm{d}\mathbf{x}' = \int \Pi\left(\frac{\mathbf{x}' - \mathbf{x}_m}{h}\right) S(\mathbf{x}' - \mathbf{x}_i)\mathrm{d}\mathbf{x}' \,, \tag{33}$$

$$\text{where:} \quad \Pi(x) = \begin{cases} 1 & \text{for } |x| \leq \frac{1}{2} \\ 0 & \text{otherwise} \end{cases}$$

Hence the mass assignment function will have the form of a convolution:

$$W(\mathbf{x}) = \Pi\left(\frac{\mathbf{x}}{h}\right) \star S(\mathbf{x}) \,. \tag{34}$$

The matter density on the grid will be the sum over the contribution from all particles described by the assignment function

$$\rho(\mathbf{x}_m) = \frac{1}{h^3} \sum_{i=1}^{N} m_i W(\mathbf{x}_i - \mathbf{x}_m) \,, \tag{35}$$

where m_i is the mass of the i-th particle. There are three commonly used shape functions $S(x)$:

$$\text{NGP:} \quad S(\mathbf{x}) = \delta_D(\mathbf{x}) \,, \tag{36}$$

$$\text{CIC:} \quad S(\mathbf{x}) = \frac{1}{h^3}\Pi(\frac{\mathbf{x}}{h}) \star \delta_D(\mathbf{x}) \,, \tag{37}$$

$$\text{TSC:} \quad S(\mathbf{x}) = \frac{1}{h^3}\Pi(\frac{\mathbf{x}}{h}) \star \frac{1}{h^3}\Pi(\frac{\mathbf{x}}{h}) \,, \tag{38}$$

where $\delta_D(\mathbf{x})$ is the Dirac delta function and the acronyms mean: NGP – *Nearest Grid Point*, CIC – *Clouds In Cells* and TSC – *Triangular Shaped Cloud*. The CIC and TSC schemes are the most popular. A simplistic NGP scheme is rarely used since it is prone to growing fluctuations. Here even a small change of a particle position can lead to a significant change in the force exerted on the particle (Potter, 1977).

Once we have the mass density $\rho(\mathbf{x}_m)$ extrapolated on a regular lattice, we can use the Discrete Fast Fourier Transform (DFFT) to obtain the equivalent density in the Fourier space, $\rho(\mathbf{k}_m)$. Multiplying the result by a suitable Green's function and doing an inverse Fourier transform gives us a real-space gravitational potential computed at all grid cells $\mathbf{x}_m$. Now using the finite difference method we can compute a force field generated by this potential:

$$\mathcal{F} = -\nabla\Phi \,. \tag{39}$$

GADGET-2 uses a $4-$th order interpolation:

$$\mathcal{F}^{(x)}_{(i),j,k} = -\frac{4}{3}\frac{\Phi_{i+1,j,k} - \Phi_{i-1,j,k}}{2h} + \frac{1}{3}\frac{\Phi_{i+2,j,k} - \Phi_{i-2,j,k}}{4h} \,, 0 \leq i,j,k \leq M \,, \tag{40}$$

where $\mathbf{x}_m = (i,j,k)$ and components j,k of the force field $\mathcal{F}$ are obtained analogously. The subsequent force field needs to be now interpolated back at each particle's position.

$$F(\mathbf{x}_i) = \sum_m W(\mathbf{x}_i - \mathbf{x}_m)\mathcal{F}_m \,. \tag{41}$$

It is crucial to use here the same interpolation scheme W as was used for the density assignment. This will ensure momentum conservation and will make the forces anti-symmetric.

3.1.2 Hierarchical tree method

The particle mesh method described in the previous section has a force resolution limited to the size h of a single mesh cell. Hence on scales $\sim \mathcal{O}(h)$ and smaller this method cannot provide faithful results. One of the alternative methods that allows for a better accuracy is the method based on a tree algorithm. In this approach the particles are organised in hierarchical groups. The force exerted on a given particle by some distant particle group is approximated by low-order multipole moments of that group. By using this approximation the number of needed computations is reduced to $\mathcal{O}(N \log N)$ (Appel, 1985), which is a significant improvement compared with $\mathcal{O}(N^2)$ operations needed in the direct particle summation method. The more terms in the multipole expansion we include during force calculation, the smaller the error of the final force. From a computational efficiency point of view, it is more beneficial to cut

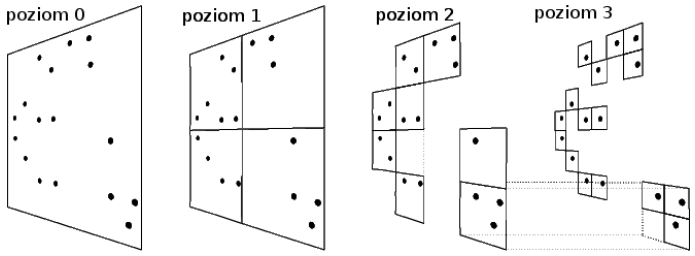

Fig. 1: A diagram illustrating construction of a Barnes&Hut tree in two dimensions. Motived by Springel et al. (2001).

the expansion at lower moments and use more leaves of the tree to reach the desired accuracy of force approximation (McMillan & Aarseth, 1993). In the GADGET-2 code a compromise between the accuracy and efficiency is reached by stopping the multipole expansion at the quadrupole term.

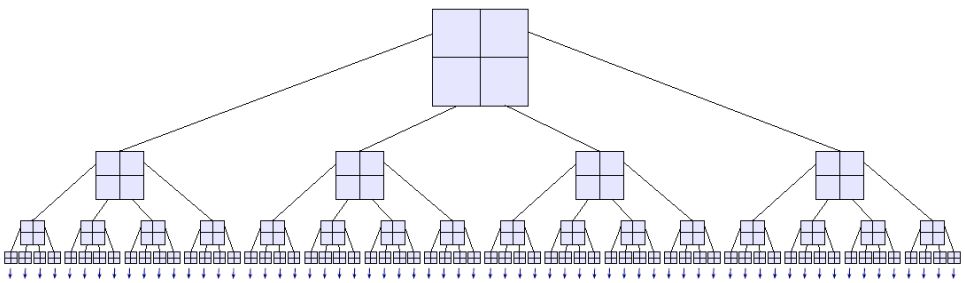

Fig. 2: A hierarchical tree structure schema. This two-dimensional analogy of a three-dimensional oct-tree is a quad-tree. Here each leaf can have at most four descendants. In 3D case the descendant number is limited to eight.

In our working example of GADGET-2, the particle tree is constructed using the method described in Barnes & Hut (1986). The computational domain is hierarchically dissected into a series of cubes. Each cube have eight descendants with their box width equal to the half of the parent width. The resulting cubes creates an oct-tree. The construction of the particle tree is made such that each leaf (cube) contains only one particle or becomes a progenitor of descendant leaves. In the latter case, in addition to the information about its descendants, the tree node also carries information about the monopole and quadrupole moments of the all particles it contains. The Fig. 1 illustrates schematically the mechanism of the tree construction. In Fig. 2 we show a two-dimensional analogue of the Barnes-Hut tree structure.

To compute the forces acting upon particles we walk the tree and add-up contributions from each consecutive tree node. In the classical Barnes-Hut algorithm the multipole expansion of a node of size l is used as a force contribution, when the

following criterion is satisfied:

$$r > \frac{l}{\theta}\,, \tag{42}$$

where r is the distance of a reference point from the centre of mass of a given tree node, while θ is an *a priori* set parameter (the so-called "opening angle") related to targeted force accuracy. When a given tree node satisfies the above condition the tree walk stops here, otherwise the node is "open" and the tree walk continues into all its descendants. The gravitational potential induced by a group of particles contained in a tree node is given by:

$$\Phi(\mathbf{r}) = -G\sum_i \frac{m_i}{|\mathbf{x_i} - \mathbf{r}|}\,, \tag{43}$$

where $\mathbf{x_i}$ is the i-th particle position vector. Let $\mathbf{s}$ be a vector pointing at the centre of mass of a particle group, and will be defined as:

$$\mathbf{s} = \frac{\sum_i m_i \mathbf{x_i}}{\sum_i m_i}\,. \tag{44}$$

Now assuming that $|\mathbf{x_i} - \mathbf{s}| \ll |\mathbf{r} - \mathbf{s}|$ holds, we can use the multipole expansion of the term:

$$\frac{1}{|\mathbf{x_i} - \mathbf{r}|} = \frac{1}{|(\mathbf{x_i} - \mathbf{s}) - (\mathbf{r} - \mathbf{s})|}\,. \tag{45}$$

By defining additionally that

$$\mathbf{y} \equiv \mathbf{r} - \mathbf{s}\,, \tag{46}$$

we will get up to the quadrupole term:

$$\frac{1}{|-\mathbf{y} + \mathbf{x_i} - \mathbf{s}|} = \frac{1}{|\mathbf{y}|} - \frac{\mathbf{y}\cdot(\mathbf{x_i} - \mathbf{s})}{|\mathbf{y}|^3} + \frac{1}{2}\frac{\mathbf{y}^T\left[3(\mathbf{x_i} - \mathbf{s})(\mathbf{x_i} - \mathbf{s})^T - \mathbf{I}(\mathbf{x_i} - \mathbf{s})^2\right]\mathbf{y}}{|\mathbf{y}|^5} + \ldots \tag{47}$$

Here ^{T} marks the transposition operation and $\mathbf{I}$ is a unitary matrix. If we will sum over all the particles the dipole term will vanish, and thus:

$$\frac{\mathbf{y}\cdot(\mathbf{x_i} - \mathbf{s})}{|\mathbf{y}|^3} = 0\,. \tag{48}$$

We can now define the remaining terms of the expansion:

$$\text{monopole:}\quad M = \sum_i m_i\,, \tag{49}$$

$$\text{quadrupole:}\quad \mathbf{K} = 3\mathbf{Q} - \mathbf{P}\,, \tag{50}$$

where the adequate tensors $\mathbf{Q}$ and $\mathbf{P}$ are given by

$$\mathbf{Q} \equiv \sum_i m_i(\mathbf{x_i} - \mathbf{s})(\mathbf{x_i} - \mathbf{s})^T = \sum_i m_i \mathbf{x_i}\mathbf{x_i}^T - M\mathbf{s}\mathbf{s}^T\,, \tag{51}$$

$$\mathbf{P} \equiv \mathbf{I}\sum_i m_i(\mathbf{x_i} - \mathbf{s})^2 = \mathbf{I}\left[\sum_i m_i \mathbf{x_i}^2 - M\mathbf{s}^2\right]\,. \tag{52}$$

Synthesizing equations from (43) to (52) will lead to this equation for the potential produced by the particles in a given tree node:

$$\Phi(\mathbf{r}) = -G\left[\frac{M}{y} + \frac{1}{2}\mathbf{y}^T\frac{\mathbf{K}}{y^5}\mathbf{y}\right] . \tag{53}$$

Therefore the final quadrupole approximation for the purely Newtonian gravitational force field is:

$$\mathbf{f}(\mathbf{r}) = -\nabla\Phi(\mathbf{r}) = G\left(-\frac{M}{y^3}\mathbf{y} + \frac{3\mathbf{Q}}{y^5}\mathbf{y} - \frac{15}{2}\frac{\mathbf{y}^T\mathbf{Q}\mathbf{y}}{y^7}\mathbf{y} + \frac{3}{2}\frac{\mathbf{P}}{y^5}\mathbf{y}\right) . \tag{54}$$

The above equation is a good approximation to the force on scales r, when we consider a pure Newtonian force. However, as already mentioned, in N-body simulations we use gravitational softening to impose colisionless dynamics. This can lead to some technical difficulties. In regions with a high particle number density (such as a DM halo core or a cold molecular hydrogen cloud) we can have a tree node that simultaneously meets the opening angle criterion (42) and also will have $r < \varepsilon$ (where ε is the gravitational softening parameter). In such a case, for the approximation to be formally correct one should use a multipole expansion of the softened potential instead of the described pure Newtonian approximation For completeness we will also briefly discuss the appropriate expansion of a smoothed potential. In general, the smoothed gravitational potential can be written as:

$$\Phi(\mathbf{r}) = -G\sum_i m_i\, g(|\mathbf{x_i} - \mathbf{r}|) , \tag{55}$$

where the function $g(r)$ describes the smoothed force law. For $g(r) = 1/r$ we will recover the standard Newtonian potential. GADGET-2 uses a relatively complicated form of the function $g(r)$, which takes form of a parametric function based on a normalized spline interpolation kernel widely used in the SPH formalism. We give the exact forms of the smoothing kernels and their derivatives in the Appendix. Now, conducting the multipole expansion in an analogous way as for the Newtonian potential will gives us an expression for the approximate smoothed potential:

$$\Phi(\mathbf{r}) = -G\left\{Mg(y) + \frac{1}{2}\mathbf{y}^T\left[\frac{g''(y)}{y^2}\mathbf{Q} + \frac{g'(y)}{y^3}(\mathbf{P} - \mathbf{Q})\right]\mathbf{y}\right\} . \tag{56}$$

Finally, the smoothed gravitational force exerted by a group of particles contained in a tree node will be, to a quadrupole approximation, given by:

$$\mathbf{f}(\mathbf{r}) = -\nabla\Phi(\mathbf{r}) = G\left[Mg_1(y)\mathbf{y} + g_2(y)\mathbf{Q}\mathbf{y} + \frac{1}{2}g_3(y)(\mathbf{y}^T\mathbf{Q}\mathbf{y})\mathbf{y} + \frac{1}{2}g_4(y)\mathbf{P}\mathbf{y}\right] , \tag{57}$$

where the functions $g1(y), g_2(y), g_3(y)$ and $g_4(y)$ are introduced as a convenient notation for the combination of derivatives of $g(y)$. We give the definitions of these functions in the Appendix (equations from (94) to (101)).

3.1.3 Combining tree and mesh – the hybrid method

As mentioned earlier, GADGET-2 combines the two numerical methods described above to obtain accurate gravitational forces. Thanks to a suitable connection of both

algorithms we get an effective and numerically optimal method that can attain, in principle, an arbitrarily high force resolution. In N-body simulations performed in a cosmological context one usually imposes periodic boundary conditions. This reflects the fact that a finite-size computational domain (usually a cube) is only a small section of an otherwise spatially-infinite Universe. The finite box size introduces the lower limit of a given simulation's dynamical range. The phenomena and structures on scales of the order of $r \gtrsim L$ (where L is the width of the computational domain) are not accessible. The implementation of periodic boundary conditions can be problematic for the case of tree algorithms. However such boundaries are naturally obtained in the case of methods using the DFFT, hence the particle mesh algorithm. We will now describe how, specifically, GADGET-2 combines the tree and mesh methods together.

The interaction potential $\varphi(\mathbf{x})$ in a box of size L, with periodic boundary conditions, is a solution of the following equation (Springel, 2005):

$$\nabla^2\varphi(\mathbf{x}) = 4\pi G\left[\sum_{\mathbf{n}}\tilde{\delta}(\mathbf{x}-\mathbf{n}L) - L^{-3}\right], \tag{58}$$

where the sum $\mathbf{n} = (n_1, n_2, n_3)$ is over all triplets of integer numbers, while the single particle distribution function $\tilde{\delta}(\mathbf{x})$ is Dirac's delta function convolved with a normalised SPH smoothing kernel (see Appendix, Eqn. (90)). In the above Poisson equation we already eliminated the averaged density, so its solution describes only the pure peculiar potential.The global dynamics of the system is described by a general Poisson equation $\nabla^2\Phi(\mathbf{x}) = 4\pi G(\rho(\mathbf{x}-\overline{\rho}))$. For a finite discrete set of particles, the peculiar potential is defined by:

$$\Phi(\mathbf{x}) = \sum_i m_i\varphi(\mathbf{x}-\mathbf{x_i})\,. \tag{59}$$

This can be written in Fourier space as:

$$\Phi_{\mathbf{k}} = -\frac{4\pi G}{\mathbf{k}^2}\rho_{\mathbf{k}}\,,\ \text{where}\ \mathbf{k}\neq 0\,. \tag{60}$$

Now we can explicitly split the above potential into a sum of two contributions, the short and long range:

$$\Phi_{\mathbf{k}} = \Phi_{\mathbf{k}}^{\text{long}} + \Phi_{\mathbf{k}}^{\text{short}}\,. \tag{61}$$

We can write the specific terms as:

$$\Phi_{\mathbf{k}}^{\text{long}} = \Phi_{\mathbf{k}}\exp(-\mathbf{k}^2r_p^2)\,, \tag{62}$$

$$\Phi_{\mathbf{k}}^{\text{short}} = \Phi_{\mathbf{k}}\left[1-\exp(-\mathbf{k}^2r_p^2)\right], \tag{63}$$

where r_p defines the scale of force split. The long-range contribution can be obtained via the particle mesh method.

The short-range part of the potential (59) can be obtained in real space when we notice that for $r_p \ll L$ this contribution can be expressed as:

$$\Phi^{\text{short}}(\mathbf{x}) = -G\sum_i\frac{m_i}{r_i}\text{erfc}\left(\frac{r_i}{2r_p}\right). \tag{64}$$

Above, the $r_i = \min(|\mathbf{x} - \mathbf{r_i} - \mathbf{n}L|)$ can be understood as the minimal distance of any i-th particle image from the reference point $\mathbf{x}$. The erfc function strongly suppresses forces on distance scales large compared to r_p, thus only the closest image of a given particle will contribute to the short-range force.

The short-range contributions to the particle forces described by the Eqn. (64) can be calculated using the Barnes-Hut tree multipole expansion method. There are additional advantages of this approach. Firstly, to get the short-range contribution of a force exerted on a given particle we need to walk only those tree nodes which are located near to the given particle. Secondly, since we only compute short-range forces by the tree method, we do not need to implement the periodic boundary conditions (those are already taken into account with the long-range contribution from the particle mesh). This speeds up the tree calculations.

3.2 Numerical hydrodynamics

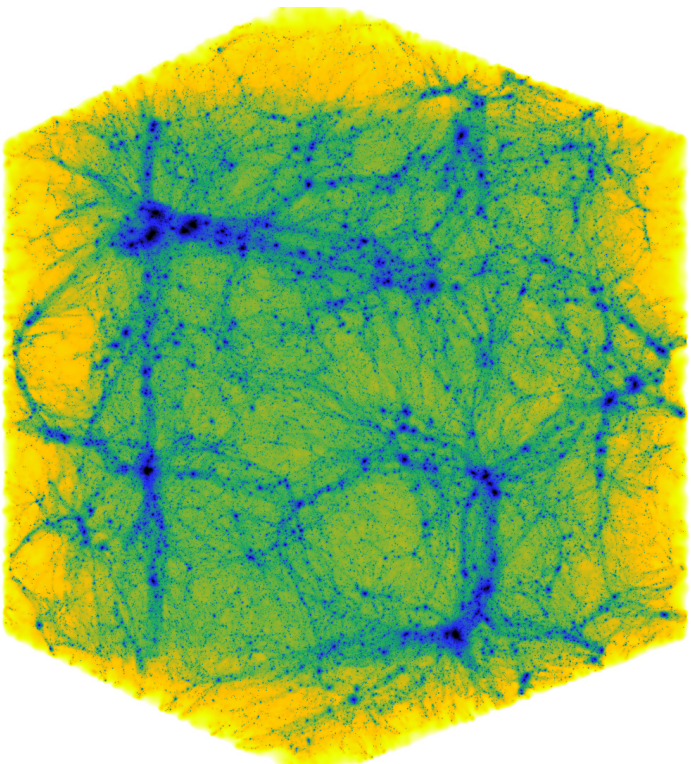

Fig. 3: A DM density rendering from the COLOR cosmological N-body simulation taken at the final stage of the simulation. The picture illustrates the high complexity of the large-scale structure and a plethora of highly clustered gravitationally bound objects. See details in Hellwing et al. (2015).

Having implemented methods for simulating a collisionless self-gravitating fluid

we are able to run simulations tracing the dynamics of the dark matter component alone. This is a commonly adopted approach, as DM-only simulations are cheap and relatively simple. Such simulations are very useful as they provide rich information about non-linear physics of gravitational clustering (see e.g. Fig. 3). However there are a number of phenomena that can only be modelled realistically when we include hydrodynamical interactions which are important for baryonic gas at galaxy scales. We are going now to discuss the basic hydro module implemented in GADGET-2.

The code uses simple prescription for intergalactic and interstellar baryonic gas, modelling it approximately as ideal non-viscous gas. Such a fluid satisfies the following continuity:

$$\frac{\mathrm{d}\rho}{\mathrm{d}t} + \rho\nabla\cdot\mathbf{v} = 0\,, \tag{65}$$

and Euler equation:

$$\frac{\mathrm{d}v}{\mathrm{d}t} = -\frac{\nabla P}{\rho} - \nabla\Phi\,. \tag{66}$$

Here ρ is the gas density, P its pressure and Φ is the gravitational potential. In addition we will have that the internal energy (heat) u per mass unit will evolve according to the first law of thermodynamics, *videlicet*:

$$\frac{\mathrm{d}u}{\mathrm{d}t} = -\frac{P}{\rho}\nabla\cdot\mathbf{v} - \frac{\Theta(u,\rho)}{\rho}\,. \tag{67}$$

In the above notation we have used the Lagrangian time derivative, i.e.:

$$\frac{\mathrm{d}}{\mathrm{d}t} = \frac{\partial}{\partial t} + \mathbf{v}\cdot\nabla\,, \tag{68}$$

and we have parametrised any allowed additional gas physics in the form of the cooling function $\Theta(u,\rho)$, which describes external heat sinks and sources. For an ideal gas the equation of state is given as:

$$P = (\gamma-1)\rho u\,, \tag{69}$$

where γ is the adiabatic index (equal to the specific heat ratio). For a single molecular gas (as interstellar gas is usually approximated) $\gamma = 5/3$. In addition, we can define the adiabatic gas sound speed:

$$c_s^2 = \gamma\frac{P}{\rho}\,. \tag{70}$$

GADGET-2 uses smoothed particle hydrodynamics to describe the physical properties of the baryonic gas. In this approach discrete tracers, like particles, are used to describe the fluid local state, while the continuous quantities are defined with a help of specific interpolation smoothing kernels (Gingold & Monaghan, 1977; Lucy, 1977). The particles with coordinates, r_i, velocities, v_i and masses, m_i, are identified as fluid elements and they trace the fluid in the Lagrangian sense. The thermodynamical state of each fluid element can be defined via its internal energy,u_i, expressed per unit mass or by the entropy, s_i, per unit mass. GADGET-2 uses the entropy in a specific formulation described in Springel & Hernquist (2002). This formulation not only assures the conservation of energy, but it also conserves the gas entropy.

Let us notice that, from the numerical point of view, it is convenient to operate with the entropy function defined as $A \equiv P/\rho^\gamma$, rather than using the entropy per unit

mass, s_i, itself. For an ideal gas A is the function of the entropy only, so $A = A(s)$. It is cheaper to compute A than the specific entropy s_i.

The most fundamental part of each SPH implementation is the estimation of local density. GADGET-2 uses the following prescription for that:

$$\rho_i = \sum_j m_j W_{SPH}(|\mathbf{r_{ij}}|, h_i)\,, \tag{71}$$

where $\mathbf{r_{ij}} \equiv \mathbf{r_i} - \mathbf{r_j}$, and the smoothing kernel $W_{SPH}(r, h)$ is given by Eqn. (90) in the Appendix. Here, the adaptive smoothing length is marked as h rather than ε to underline the fact that this parameter has a different meaning than the gravitational softening parameter. For each particle individually its smoothing length, h_i, is defined so that the volume of the corresponding smoothing kernel contains a fixed mass at pre-set density. Hence, implicitly, the length and the density associated with a particle satisfies:

$$\frac{4\pi}{3} h_i^3 \rho_i = N_{SPH} \overline{m}\,, \tag{72}$$

where N_{SPH} is the typical number of nearest neighbours used for smoothing, and $\overline{m}$ is the averaged mass of the particle.

Springel and Hernquist showed that, in the discrete fluid Lagrangian formalism, the equations of motion of SPH particles are given by (Springel & Hernquist, 2002):

$$\frac{\mathrm{d}v_i}{\mathrm{d}t} = -\sum_j m_j \left[f_i \frac{P_i}{\rho_i^2} \nabla_i W_{ij}(h_i) + f_j \frac{P_j}{\rho_j^2} \nabla_i W_{ij}(h_j) \right], \tag{73}$$

where f_i factors are defined as:

$$f_i = \left(1 + \frac{h_i}{3\rho_i} \frac{\partial \rho_i}{\partial h_i} \right)^{-1}, \tag{74}$$

and we have also used the simplified notation $W_{ij}(h) = W_{SPH}(|\mathbf{r_i} - \mathbf{r_j}|, h)$. Finally the pressure associated with particles can be expressed as:

$$P_i = A_i \rho_i^\gamma\,. \tag{75}$$

The system of equations presented above describes fluid dynamics in the SPH formalism. For such a flow the entropy A_i associated with each individual particle is conserved. This is true as long as there are no shocks or external heat sources in the gas.

It is known, however, that the flow of an ideal gas can generate discontinuities, in which entropy grows due to the microphysics of gas. In the SPH method we capture such shock-containing regions by artificial viscosity. GADGET-2 uses the following prescription for the viscous fluid force:

$$\left.\frac{\mathrm{d}v_i}{\mathrm{d}t}\right|_{\text{viscous}} = -\sum_j m_j \Pi_{ij} \nabla_i \overline{W}_{ij}\,, \tag{76}$$

where the viscosity term $\Pi_{ij} \geq 0$ has non-zero value only for pairs of particles, which approach each other in physical space. Viscosity generates entropy at a rate:

$$\frac{\mathrm{d}A_i}{\mathrm{d}t} = \frac{1}{2} \frac{\gamma - 1}{\rho_i^{\gamma-1}} \sum_j m_j \Pi_{ij} \mathbf{v}_{ij} \cdot \nabla_i \overline{W}_{ij}\,, \tag{77}$$

dissipating gas kinetic energy into heat. In the above two equations we have used the $\overline{W}_{ij}$ symbol to mark the arithmetic average from two smoothing kernels $W_{ij}(h_i)$ and $W_{ij}(h_j)$. GADGET-2 specifically implements viscosity as described by the ansatz (Monaghan, 1997):

$$\Pi_{ij} = -\frac{\alpha}{2}\frac{w_{ij}v_{ij}^{\mathrm{syg}}}{\rho_{ij}}\,, \tag{78}$$

where the signal velocity in the simplest form takes:

$$v_{ij}^{\mathrm{syg}} = c_i + c_j - 2w_{ij}\,. \tag{79}$$

Here $w_{ij} = v_{ij}\cdot\mathbf{r}_{ij}/|\mathbf{r}_{ij}|$ is the relative particle velocity projected onto the particle separation vector, provided that the particles approach each other (hence $v_{ij}\cdot\mathbf{r}_{ij} < 0$). Otherwise we set $w_{ij} = 0$. c_i and c_j marks the average sound speed. The α parameter regulates the strength of the viscous forces. Substituting Eqn. (79) into Eqn. (78) we will get the final form of the viscosity term:

$$\Pi_{ij} = -\frac{\alpha}{2}\frac{(c_i + c_j - 3w_{ij})w_{ij}}{\rho_{ij}}\,. \tag{80}$$

Following the SPH dynamics using the above methods we obtain additional hydrodynamical forces acting on each particle. Since force, being a vector, follows the superposition principle, the hydrodynamical force contribution can just be added to the gravitational part for all particles representing baryonic matter and used to obtain the total acceleration of a given particle. In addition this simple description can be developed further by introducing extra bits of baryonic physics (like start formation, energetic stellar feedback or Active Galactic Nuclei) (see e.g. Crain et al., 2009; Vogelsberger et al., 2014; Schaye et al., 2015).

3.3 Time integration of equations of motion

The forces calculated in cosmological N-body simulations are not very accurate, and may not be smooth and continuous. This favours low order integration schemes. In contrast, in modelling of orbital dynamics high order integrators are used. It is crucial that our integration scheme uses Hamiltonian operators. Non-Hamiltonian operators have unwanted properties such as, for example, poor energy conservation.

A system N-body of particles can be described by a separable Hamiltonian function:

$$\mathbf{H} = \mathbf{H_{kin}} + \mathbf{H_{pot}}\,. \tag{81}$$

Here $\mathbf{H_{kin}}$ will describe the kinetic energy part of the system and $\mathbf{H_{pot}}$ the potential energy. No we can introduce a pair of time operators that will act on different terms in our separable Hamiltonian, the kick and drift time operators:

$$\mathbf{D}(\Delta t) \equiv \exp\left(\int_t^{t+\Delta t} \mathrm{d}t\;\mathbf{H_{kin}}\right)\begin{cases} p_i \to p_i, \\ x_i \to x_i + \frac{p_i}{m_i}\Delta t. \end{cases} \tag{82}$$

$$\mathbf{K}(\Delta t) \equiv \exp\left(\int_t^{t+\Delta t} \mathrm{d}t\;\mathbf{H_{pot}}\right)\begin{cases} x_i \to x_i, \\ p_i \to p_i - \sum_j m_i m_j \frac{\partial\phi(x_{ij})}{\partial x_i}\Delta t. \end{cases} \tag{83}$$

As indicated above, the drift operator updates particles positions using predicted velocity, while the kick operator updates particles momenta using predicted forces. Here for simplicity we have written only the spatial gradient of the peculiar potential $\phi(x_{ij})$, which gives the gravitational forces. In general, when we also model the hydrodynamics the adequate hydro forces should also be included here. Both these operators can be combined together to create very efficient time integration schemes. Usually one considers two variations: the Drift-Kick-Drift (DKD) and Kick-Drift-Kick (KDK) schemes:

$$\tilde{\mathbf{U}}(\Delta t) = \mathbf{D}\left(\frac{\Delta t}{2}\right)\mathbf{K}(\Delta t)\mathbf{D}\left(\frac{\Delta t}{2}\right) \tag{84}$$

$$\tilde{\mathbf{U}}(\Delta t) = \mathbf{K}\left(\frac{\Delta t}{2}\right)\mathbf{D}(\Delta t)\mathbf{K}\left(\frac{\Delta t}{2}\right) \tag{85}$$

$$\tag{86}$$

At the end, we also need to ensure sufficiently accurate time integration of the whole N-body system. If our time integration is not accurate enough, then even after a small number of time steps we will obtain completely non-physical behaviour of our system. The most stable and accurate solutions are obtained usually by using the KDK scheme with variable (adaptive) time steps.

3.4 Initial conditions

At the end of our short introduction to numerical techniques used commonly in cosmological N-body simulations we will describe one of the methods that is used to generate the initial conditions. Accurate initial conditions are very important, as for highly non-linear systems the error in initial particles positions and velocities can lead to significantly different end-state results.

The predictions of linear perturbation theory for large-scale structure are usually encoded in a form of the 3D power spectrum of spatial density fluctuations. Such a power spectrum can be written as the combination of a primordial post-inflationary spectrum of fluctuations and the so-called transfer function, which describes late-time linear evolution of each density Fourier mode. A power-law inflationary spectrum is commonly adopted together with a random initial Gaussian phases, and the specific transfer functions for a given cosmology can be computed explicitly (see e.g. Peacock & Dodds, 1996; Eisenstein & Hu, 1999; Smith et al., 2003).

The problem of generating the initial conditions is then reduced to generating adequate random phases which are the realisation of an initial random field and a given power spectrum, and displacing N-body particles inside a computational domain. In the real, infinite Universe the Fourier power spectrum of fluctuations is continuous and hence the assumption of random phases implies that the density in any arbitrarily chosen point has a Normal distribution. In numerical simulations the model of the Universe has a finite size and so the Fourier spectrum is discrete. In this case the random phases assumption is not enough to assure a Gaussian density distribution. We need to make the additional assumption that the amplitude of each mode also has a Normal distribution, with a variance equivalent to the expected amplitude of a given mode. Only with this assumption will we get a frequency of high-density peaks (*exempli gratia* 2 or 3 σ) in an ensemble of a given input power spectrum realisation

which is the same as the frequency of such peaks in a real, infinite universe with a continuous power spectrum.

A convenient and effective method to generate initial conditions that realize an arbitrary initial power spectrum can be obtained from the Lagrangian formalism describing the linear evolution of a general distribution of fluctuations, first derived by Yakov Zeldovitch (Zel'Dovich, 1970):

$$\mathbf{x}(t) = \mathbf{q} - D(t)\psi(\mathbf{q})\,, \tag{87}$$

Here $\mathbf{x}$ is the final comoving particle position vector in Eulerian space, $\mathbf{q}$ is the Lagrangian initial position, $D(t)$ describes the growth rate of linear perturbations and ψ defines the spatial density fluctuation field. The field ψ can be express in terms of a force field for a given time t:

$$\psi(\mathbf{q}) = -\frac{\mathbf{F}(\mathbf{q},t)}{ma^2(a\ddot{D} + 2\dot{D}\dot{a})}\,. \tag{88}$$

If we create a power spectrum realisation in Fourier space by generating random Gaussian amplitudes and phases, we can multiply them with an adequate Green's function to get the corresponding peculiar gravitational potential sampled on a regular lattice. By differentiating and interpolating back onto the grid this potential will give us the values of the force field $\mathbf{F}(\mathbf{q},t)$. We can use here exactly the same steps as in the previously-described particle mesh method (see § 3.1). Now equations (87) and (88) completely describe the perturbed particle positions that we need to obtain the desired density field from the initial regular homogeneous particle distribution.

Once we set the initial perturbed particle positions, the next step is to calculate the corresponding initial peculiar velocities. It is worth noting here that, for starting times used in cosmological simulations ($100 \lesssim z \lesssim 20$), we can expect that only the fastest-growing density modes will be present in the Universe at those early times. Under this assumption we can obtain particle initial velocities by differentiating Eqn. (87):

$$\dot{\mathbf{x}} = -\dot{D}\psi(\mathbf{q})\,. \tag{89}$$

The simplest way to compute such a velocity field is to use Eqn. (88) and (89) together with the force field we calculated to perturb particle positions. Once we have particle initial positions and velocities we are ready to start the N-body simulation and run numerical experiments to study the non-linear regime of cosmic large-scale structure formation.

Appendix - numerical smoothing kernels

The smoothing kernel used in GADGET-2 SPH code is a spline function of the following shape (Monaghan & Lattanzio, 1985):

$$W_{SPH}(r;\varepsilon) = \frac{8}{\pi\varepsilon^3}\begin{cases} 1 - 6\left(\frac{r}{\varepsilon}\right)^2 + 6\left(\frac{r}{\varepsilon}\right)^3\,, & 0 \le \frac{r}{\varepsilon} \le \frac{1}{2}\,, \\ 2(1-\frac{r}{\varepsilon})^3\,, & \frac{1}{2} < \frac{r}{\varepsilon} \le 1\,, \\ 0\,, & \frac{r}{\varepsilon} > 1\,. \end{cases} \tag{90}$$

Here r is the distance between particles, and ε is the softening parameter.

The smoothed gravitational potential of a particle group contained in a tree node is given by (see also Eqn. (55)):

$$\Phi(\mathbf{r}) = -G \sum_i m_i \, g(|\mathbf{x_i} - \mathbf{r}|) \,. \tag{91}$$

If we treat the force exerted by a point-like mass m_i as a force coming from an equivalent continuous density distribution $\rho(\mathbf{r}) = m_i W_{SPH}(\mathbf{r}; \varepsilon)$, then the resulting smoothing function $g(r)$ will be (Springel et al., 2001):

$$g(r) = -\frac{1}{\varepsilon} W_g \left(\frac{r}{\varepsilon} \right) . \tag{92}$$

Here the smoothing kernel is given by:

$$W_g(u) = \begin{cases} \frac{16}{3}u^2 - \frac{48}{5}u^4 + \frac{32}{5}u^5 - \frac{14}{5} \,, & 0 \le u \le \frac{1}{2} \,, \\ \frac{1}{15u} + \frac{32}{3}u^2 - 16u^3 + \frac{48}{5}u^4 - \frac{32}{15}u^5 - \frac{16}{5} \,, & \frac{1}{2} \le u < 1 \,, \\ -\frac{1}{u} \,, & u \ge 1 \,. \end{cases} \tag{93}$$

The derivatives of the function $g(r)$ appear in the multipole expansion of a smoothed gravitational potential. These functions, used in Eqn. (57), have the following specific forms:

$$g_1(y) = \frac{g'(y)'}{y} \,, \tag{94}$$

$$g_2(y) = \frac{g''(y)}{y^2} - \frac{g'(y)}{y^3} \,, \tag{95}$$

$$g_3(y) = \frac{g_2'(y)}{y} \,, \tag{96}$$

$$g_4(y) = \frac{g_1'(y)}{y} \,. \tag{97}$$

By assuming $u = y/\varepsilon$, we can write down the above functions explicitly as:

$$g_1(y) = \frac{1}{\varepsilon^3} \begin{cases} -\frac{32}{3} + \frac{192}{5}u^2 - 32u^3 \,, & u \le \frac{1}{2} \,, \\ \frac{1}{15u^3} - \frac{64}{3} + 48u - \frac{192}{5}u^2 + \frac{32}{3}u^3 \,, & \frac{1}{2} < u < 1 \,, \\ -\frac{1}{u^3} \,, & u > 1 \,, \end{cases} \tag{98}$$

$$g_2(y) = \frac{1}{\varepsilon^5} \begin{cases} \frac{384}{5} - 96u \,, & u \le \frac{1}{2} \,, \\ -\frac{384}{5} - \frac{1}{5u^2} + \frac{48}{u} + 32u \,, & \frac{1}{2} < u < 1 \,, \\ \frac{3}{u^5} \,, & u > 1 \,, \end{cases} \tag{99}$$

$$g_3(y) = \frac{1}{\varepsilon^7} \begin{cases} -\frac{96}{u} \,, & u \le \frac{1}{2} \,, \\ \frac{32}{u} + \frac{1}{u^7} - \frac{48}{u^3} \,, & \frac{1}{2} < u < 1 \,, \\ -\frac{15}{u^7} \,, & u > 1 \,, \end{cases} \tag{100}$$

$$g_4(y) = \frac{1}{\varepsilon^7} \begin{cases} -\frac{96}{5}(5u - 4) \,, & u \le \frac{1}{2} \,, \\ \frac{48}{u} - \frac{1}{5u^5} - \frac{384}{5} + 32u \,, & \frac{1}{2} < u < 1 \,, \\ \frac{3}{u^5} \,, & u > 1 \,. \end{cases} \tag{101}$$

References

Appel, A. W., *An Efficient Program for Many-Body Simulation*, *SIAM Journal on Scientific and Statistical Computing* **6**, 1, 85 (1985), URL `http://link.aip.org/link/?SCE/6/85/1`

Barnes, J., Hut, P., *A hierarchical O(N log N) force-calculation algorithm*, Nature **324**, 446 (1986)

Bennett, C. L., et al., *Cosmic temperature fluctuations from two years of COBE differential microwave radiometers observations*, ApJ **436**, 423 (1994), astro-ph/9401012

Bennett, C. L., et al., *Four-Year COBE DMR Cosmic Microwave Background Observations: Maps and Basic Results*, ApJ **464**, L1+ (1996), astro-ph/9601067

Boltzmann, L., *Weitere Studien über das Wärmegleichgewicht unter Gasmolekülen*, *Wiener Berichte* **66**, 275 (1872)

Crain, R. A., et al., *Galaxies-intergalactic medium interaction calculation - I. Galaxy formation as a function of large-scale environment*, MNRAS **399**, 1773 (2009), astro-ph/0906.4350

Dodelson, S., Modern Cosmology, Academic Press, Elsevier Science (2003)

Eisenstein, D. J., Hu, W., *Power Spectra for Cold Dark Matter and Its Variants*, ApJ **511**, 5 (1999), astro-ph/9710252

Gingold, R. A., Monaghan, J. J., *Smoothed particle hydrodynamics - Theory and application to non-spherical stars*, MNRAS **181**, 375 (1977)

Hellwing, W. A., et al., *The Copernicus Complexio: a high-resolution view of the small-scale Universe*, *ArXiv e-prints* (2015), astro-ph/1505.06436

Hockney, R. W., Eastwood, J. W., Computer Simulation Using Particles, McGraw-Hill, New York (1981)

Komatsu, E., et al., *Seven-Year Wilkinson Microwave Anisotropy Probe (WMAP) Observations: Cosmological Interpretation*, *ArXiv e-prints* (2010), astro-ph/1001.4538

Lucy, L. B., *A numerical approach to the testing of the fission hypothesis*, AJ **82**, 1013 (1977)

McMillan, S. L. W., Aarseth, S. J., *An O(N log N) integration scheme for collisional stellar systems*, ApJ **414**, 200 (1993)

Monaghan, J. J., *SPH and Riemann Solvers*, *Journal of Computational Physics* **136**, 298 (1997)

Monaghan, J. J., Lattanzio, J. C., *A refined particle method for astrophysical problems*, A&A **149**, 135 (1985)

Peacock, J. A., Dodds, S. J., *Non-linear evolution of cosmological power spectra*, *Mon. Not. Roy. Astron. Soc.* **280**, L19 (1996), astro-ph/9603031

Planck Collaboration, et al., *Planck 2013 results. XVI. Cosmological parameters*, A&A **571**, A16 (2014), astro-ph/1303.5076

Potter, D., Metody obliczeniowe fizyki, Państwowe Wydawnictwa Naukowe (1977)

Schaye, J., et al., *The EAGLE project: simulating the evolution and assembly of galaxies and their environments*, MNRAS **446**, 521 (2015), astro-ph/1407.7040

Smith, R. E., et al., *Stable clustering, the halo model and non-linear cosmological power spectra*, *Mon. Not. Roy. Astron. Soc.* **341**, 1311 (2003), astro-ph/0207664

Springel, V., *The cosmological simulation code GADGET-2*, *Mon. Not. Roy. Astron. Soc.* **364**, 1105 (2005), astro-ph/0505010

Springel, V., Hernquist, L., *Cosmological smoothed particle hydrodynamics simulations: the entropy equation*, MNRAS **333**, 649 (2002), astro-ph/0111016

Springel, V., Yoshida, N., White, S. D. M., *GADGET: a code for collisionless and gasdynamical cosmological simulations*, *New Astronomy* **6**, 79 (2001), astro-ph/0003162

Vogelsberger, M., et al., *Introducing the Illustris Project: simulating the coevolution of dark and visible matter in the Universe*, MNRAS **444**, 1518 (2014), `astro-ph/1405.2921`

Zel'Dovich, Y. B., *Gravitational instability: An approximate theory for large density perturbations.*, A&A **5**, 84 (1970)